Artifacts in automatic retinal segmentation using different optical coherence tomography instruments.

ARTIFACTS IN AUTOMATIC RETINAL SEGMENTATION USING DIFFERENT OPTICAL COHERENCE TOMOGRAPHY INSTRUMENTS

ANDREA GIANI, MD,* MARIO CIGADA, MD,† DANIEL D. ESMAILI, MD,‡
PAOLA SALVETTI, MD,† SAVERIO LUCCARELLI, MD,†
ERMENGARDA MARZIANI, MD,† CRISTIANO LUISELLI, MD,†
PIERFILIPPO SABELLA, MD,† MATTEO CEREDA, MD,§
CHIARA EANDI, MD,¶ GIOVANNI STAURENGHI, MD†

Purpose: The purpose of this study was to compare and evaluate artifact errors in automatic inner and outer retinal boundary detection produced by different time-domain and spectral-domain optical coherence tomography (OCT) instruments.

Methods: Normal and pathologic eyes were imaged by six different OCT devices. For each instrument, standard analysis protocols were used for macular thickness evaluation. Error frequencies, defined as the percentage of examinations affected by at least one error in retinal segmentation (EF-exam) and the percentage of total errors per total B-scans, were assessed for each instrument. In addition, inner versus outer retinal boundary delimitation and central (1,000 μm) versus noncentral location of errors were studied.

Results: The study population of the EF-exam for all instruments was 25.8%. The EF-exam of normal eyes was 6.9%, whereas in all pathologic eyes, it was 32.7% ($P < 0.0001$). The EF-exam was highest in eyes with macular holes, 83.3%, followed by epiretinal membrane with cystoid macular edema, 66.6%, and neovascular age-related macular degeneration, 50.3%. The different OCT instruments produced different EF-exam values ($P < 0.0001$). The Zeiss Stratus produced the highest percentage of total errors per total B-scans compared with the other OCT systems, and this was statistically significant for all devices ($P \leq 0.005$) except the Optovue RTvue-100 ($P = 0.165$).

Conclusion: Spectral-domain OCT instruments reduce, but do not eliminate, errors in retinal segmentation. Moreover, accurate segmentation is lower in pathologic eyes compared with normal eyes for all instruments. The important differences in EF among the instruments studied are probably attributable to analysis algorithms used to set retinal inner and outer boundaries. Manual adjustments of retinal segmentations could reduce errors, but it will be important to evaluate interoperator variability.

RETINA 30:607–616, 2010

With the ability to visualize the layered structure of the retina,[1–6] optical coherence tomography (OCT) has improved the diagnosis and management of many ocular diseases. One of its principal features is the quantitation of macular thickness, an important indicator of the severity of different pathologic conditions. Optical coherence tomography also provides the opportunity to follow the evolution of macular disease and the effectiveness of the therapies.[7–10]

From the *G. B. Bietti Eye Foundation, IRCCS, Rome, Italy; †Eye Clinic, Department of Clinical Science "Luigi Sacco," Sacco Hospital, University of Milan, Milan, Italy; ‡Retina Service, Massachusetts Eye and Ear Infirmary, Harvard Medical School, Boston, Massachusetts; §Department of Ophthalmology, Sacro Cuore Hospital of Negrar, Verona, Italy; and ¶Department of Clinical Physiopathology - Eye Clinic - University of Torino, Torino, Italy.

Andrea Giani, Saverio Luccarelli, and Giovanni Staurenghi received fees for attending a meeting from Carl Zeiss Meditec, Inc., Dublin, CA. Giovanni Staurenghi received fees for attending a meeting from Heidelberg Engineering, Heidelberg, Germany. The sponsors had no role in the design or conduct of this research.

None of the authors have any financial or conflicting interests to disclose.

Reprint requests: Andrea Giani, MD, Eye Clinic, II School of Ophthalmology, Department of Clinical Science "Luigi Sacco," Sacco Hospital, University of Milan Italy, W: via G. B. Grassi 74, 20100 Milan, Italy; e-mail: andreagiani@gmail.com

Most of the initial OCT studies used the Zeiss Stratus OCT instrument that is based on time-domain (TD) technology. With the Zeiss Stratus, the measurement of retinal thickness is determined by integrated software that sets the retinal boundaries of the OCT images, automatically defining inner and outer limits. The inner retinal limit is easily identified as the first signal from the vitreoretinal interface, whereas the outer limit is the signal from the interface layer between inner and outer segments of photoreceptors.[1] These measurements can be affected by errors that produce artifacts, particularly in those pathologic conditions that more intensely disrupt the normal shape of the retinal layers.[1,11,12,14,15] This study describes artifact errors in automated retinal segmentation and compares the error frequency (EF) of the Zeiss Stratus with five new spectral-domain (SD) OCT instruments that have important axial resolution and speed of acquisition improvements.[16,17] These new instruments were evaluated to determine whether they reduced the EF. The percentage of artifact occurrences with the severity of the pathologic condition was also correlated.

Methods

This prospective study was conducted in accordance with the ethical standards stated in the Declaration of Helsinki. The study was approved by the Sacco Hospital Ethics Committee. Each patient gave informed written consent before the OCT and retinal imaging examination.

All patients who presented to the Sacco Hospital Eye Clinic were enrolled consecutively. The only exclusion criterion was the presence of significant media opacity that made OCT examination impossible.

Each patient was classified by his or her pathologic condition and underwent complete ophthalmologic evaluation followed on the same day by OCT examination. Six different OCT instruments were used in this study: 1) the Zeiss Stratus OCT using software version 4.0.2 (Carl Zeiss Meditec, Inc., Dublin, CA); 2) the Zeiss Cirrus using software version 2.0.0.54 (Carl Zeiss Meditec, Inc.); 3) the HRA Spectralis using software version 3.1.4 (Heidelberg Engineering, Heidelberg, Germany); 4) the RTVue-100 using software Version 2.5 (Optovue, Inc., Fremont, CA); 5) the Optopol Copernicus using software version 2.01 (Optopol Technology S.A., Zawiercie, Poland); and 6) the Topcon 3D OCT-1000 using software version 2.12 (Topcon Corporation, Tokyo, Japan). The order of OCT examinations was randomly chosen for each patient and a minimum of 15 minutes elapsed between each examination. Expert and trained operators performed all the OCT examinations according to the analysis protocol and variables for each machine (Table 1). For each machine, the best achievable image quality was obtained by providing artificial tears/lubricants before each scanning session and accounting for the best-corrected visual acuity when adjusting the focus. After each examination, an expert physician (PS) analyzed the images and subjectively deemed them acceptable if the image was clearly visible and distinguishable in every B-scan; no eye movement or blinking artifacts occurred during the

Table 1. OCT Instruments and Protocols

Instrument	Protocol	Area	Scan Lines	A-Scans per B-Scan
Zeiss Stratus	Fast macular thickness map	6-mm lines, equally spaced 30° apart centered at the fovea	Six lines	128
Zeiss Cirrus	512 × 128 cube	6 × 6 mm	128 horizontal lines	512
HRA Spectralis	Volume	19 horizontal, consecutive parallel lines on area of 30° (length) per 15° (height); corresponded to a variable area of 7–9 mm per 4–5 mm, depending on the focus	Each single line resulted from real-time mean image reconstruction on 20 single frames to avoid speckle noise	1,536
Optovue RTvue-100	MM5	5 × 5 mm centered on the fovea	11 horizontal and 11 vertical lines (central 3 × 3 mm area), 6 horizontal and 6 vertical lines (central 5 × 5 mm area)	668 on 3 × 3-mm area 400 on 5 × 5-mm area
Optopol Copernicus	3D scan	7 × 7 mm	50 horizontal lines	743
Topcon 3D OCT-1000	3D acquisition	6 × 6 mm	128 horizontal lines	512

3D, three-dimensional.

examination; and the full depth and extent of the retina was visualized in each B-scan image. The quality of OCT images was also evaluated by averaging the parameters indicated in the software printouts for the 3 instruments in which such data were provided: the Zeiss Stratus OCT (parameter name: signal strength), the Zeiss Cirrus (parameter name: signal strength), and the Topcon 3D OCT-1000 (parameter name: Q factor).

At each examination, expert observers (AG, SL, MC) evaluated for the presence and characteristics of artifacts produced by the different machines in the automatic positioning of the inner and outer retinal boundaries in the macula area corresponding to the central and midareas in the Early Treatment Diabetic Retinopathy Study scheme. Artifacts were defined as any error in the positioning of retinal boundaries, both inner and outer. This definition did not include a severity scale, but did include every B-scan with a visible error or inconsistency from the real retinal boundary by ≥ 5 μm. All the OCT instruments identified the inner retinal boundary as the first interferometric signal after the vitreous hyporeflective space, which corresponds to the internal limiting membrane. There were important differences, however, between positioning of the outer retinal boundaries. The Zeiss Stratus identifies the outer boundary at the inner–outer photoreceptor junctional interface. The Topcon 3D OCT-1000 and the Copernicus OCT identify the outer boundary at the inner limit of retinal pigment epithelium layer, the Zeiss Cirrus at the middle of the retinal pigment epithelium layer, the Optovue RTvue-100 at the external limit of the retinal pigment epithelium, and the Heidelberg Spectralis at Bruch membrane.

This classification was repeated on every examination by expert observers (AG, SL). If there was disagreement, a third expert observer (MC) evaluated the case and decided the presence or absence of error. For the Zeiss Stratus, we used the retinal thickness (single eye) protocol and analyzed each single radial scan line. For the other OCT instruments, each B-scan image within the study boundary was analyzed. Images from each OCT examination were reviewed to evaluate the total number of scan lines affected by artifact, whether they affected the inner and/or outer retinal boundary, and if they occurred within the central 1,000-μm area. The examination error frequency (EF-exam) was calculated as a percentage of OCT examinations that included at least one B-scan with an artifactual error. To account for the different number of scan lines and variable B-scan density of each instrument, the absolute number of errors produced by each instrument was recorded, and the ratio of total number of errors per total number of B-scans for each machine was calculated (EF-scan).

These data were analyzed with the chi-square test and by generalized linear model binomial error (logit). For each OCT instrument, generalized linear model binomial error was computed by comparing the absolute error number with the total scan lines. First-order interactions between the instrument and the error position (central vs. noncentral and inner vs. outer) were computed. Statgraphics version 5.1 (Statistical Graphics Corp., Herndon, VA) and R language[13] statistics software were used.

Results

A total of 110 eyes in 63 patients (23 men and 40 women) were analyzed. The mean age was 65.7 years (range, 20–90 years). Thirty-one eyes were normal (28.5%), although the most frequent pathologic conditions were neovascular age-related macular degeneration (AMD) (22.3%), epiretinal membrane without foveal shape alterations (15.8%), cystoid macular edema (11.6%), and nonneovascular AMD (10.7%). Other pathology classes were too few to allow statistical analysis (Figure 1).

The Zeiss Stratus, Zeiss Cirrus, and the Topcon 3D OCT-1000 provided an image quality score for each OCT examination. The Zeiss Stratus had a mean signal strength of 6 (standard deviation 1.1), the Zeiss Cirrus a signal strength of 8.2 (standard deviation 0.9), and the Topcon 3D OCT-1000 a Q factor of 63.69 (standard deviation 13.55).

Error Frequency Evaluation

For the whole study population, including healthy subjects and patients with various pathologic conditions,

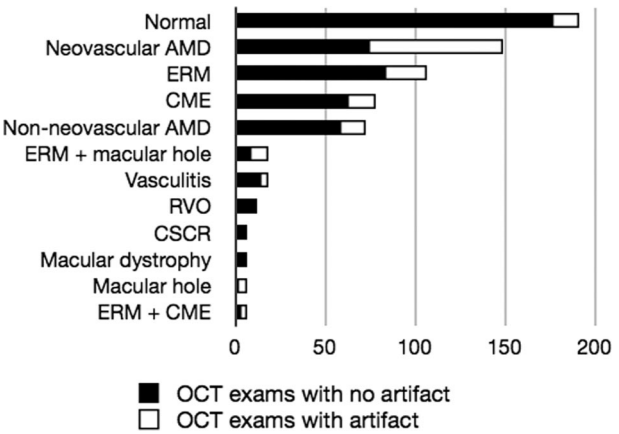

Fig. 1. Total number of examinations with and without artifacts. For all six OCT instruments, the number of errors increased with the severity of retinal alterations. The number of samples allowed statistical analysis for only healthy subjects, nonneovascular and neovascular AMD, ERM, and CME. ERM, epiretinal membrane; CME, cystoid macular edema; RVO, retinal vein occlusion; CSCR, central serous chorioretinopathy.

the total EF-exam of all OCT instruments was 25.8%. In general, the EF-exam increased with the severity and irregularity of retinal alterations. In healthy subjects, the EF-exam for all instruments was 6.9%, whereas in pathologic eyes, the EF-exam was 32.7% (chi-square, $P < 0.0001$). With severe and irregular alterations in retinal shape, the EF-exam was very high. The highest was for macular holes, 83.3%, followed by epiretinal membrane with cystoid macular edema, 66.6%, and neovascular AMD, 50.3%. With small alterations in retinal shape, the EF-exam decreased but remained higher than in normal retinas. In nonneovascular age-related maculopathy, the EF-exam was 19.4%, and in branch retinal vein occlusion, it was 8.3%.

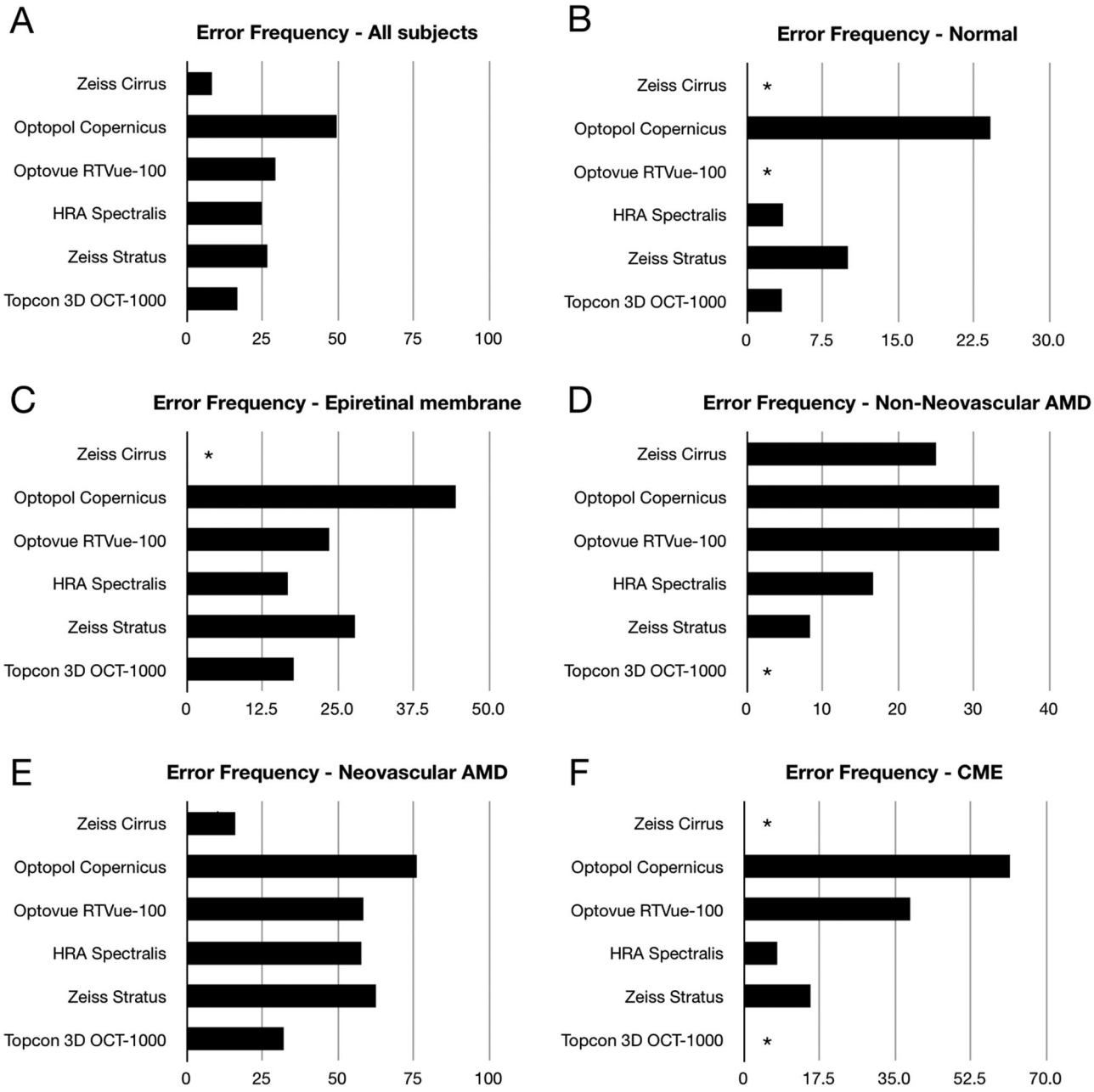

Fig. 2. Instrument-specific examination error frequencies (EF-exam): percentage of examinations affected by at least one artifact. **A,** Data from the entire sample. The Zeiss Cirrus produced the lowest value of errors. **B,** Healthy subjects. The Optovue RTvue-100 and the Zeiss Cirrus produced no errors. **C,** Epiretinal membranes without foveal shape alterations. The Zeiss Cirrus produced no errors. **D,** Patients with nonneovascular AMD. Topcon 3D OCT-1000 produced no errors. **E,** Neovascular AMD. Only the Zeiss Cirrus and Topcon 3D OCT-1000 error rates were <50%. **F,** Cystoid macular edema, including both diabetic macular edema and all other causes of primary macular edema (i.e., Irvine-Gass syndrome). The Topcon 3D OCT-1000 and Zeiss Cirrus produced no errors. *No errors were recorded.

For the study population, there was an overall difference in EF-exam among the instruments. The Zeiss Cirrus and 3D OCT-1000 instruments had the lowest EF-exam values with 8.2% and 16.6%, respectively, whereas the other devices had higher EF-exam values, varying from 24.7% for the HRA Spectralis to 49.5% for the Optopol Copernicus (Figure 2A). The Zeiss Stratus, the only TD-OCT in this study, had an EF-exam of 26.61%.

For healthy subjects (Figure 2B), the Optovue RTvue-100 and Zeiss Cirrus did not produce any errors. The Topcon 3D OCT-1000 and HRA Spectralis had very low EF-exam values, 3.45% and 3.57%, respectively. The Zeiss Stratus and Optopol Copernicus had the highest EF-exam values, 10% and 24.14%, respectively.

In eyes affected by epiretinal membranes without retinal alterations, the algorithm produced artifacts because of the membrane shape, causing it to miss the real retinal inner boundary. Although the Zeiss Cirrus never missed the inner retinal boundary, the HRA Spectralis and Topcon instruments produced errors in 16.67% and 17.65% of the examinations, respectively (Figure 2C).

In nonneovascular AMD, the alterations are in the outer retina, and the most frequent error was the identification of the shape of the retinal pigment epithelium (Figure 2D). The Topcon OCT did not produce any errors, whereas the HRA Spectralis and Zeiss Cirrus had relatively low EF-exam values, 16.67% and 25.0%, respectively. The Optopol Copernicus and Optovue RTvue-100 instruments had the highest EF-exam value, 33.33% for each. The TD-OCT Zeiss Stratus EF-exam was 8.33%. In neovascular AMD (Figure 2E), the Zeiss Cirrus and Topcon OCT instruments had the lowest EF-exam, 16.0% and 32.0%, respectively. The HRA Spectralis, Optovue RTvue-100, and Zeiss Stratus had similar EF-exams of 57.6%, 58.3%, and 62.5%, respectively. The EF-exam for the Optopol Copernicus was 76.0%.

In eyes with cystoid macular edema (Figure 2F), the Zeiss Cirrus and Topcon OCT instruments did not produce errors. The HRA Spectralis and Zeiss Stratus had similar EF-exams of 7.69% and 15.38%, respectively, and the EF-exams for Optovue RTvue-100 and Optopol Copernicus were 38.4% and 61.5%, respectively.

The Optopol Copernicus compiled the highest number of total errors compared with the other instruments, whereas the Topcon OCT exhibited the fewest (Figure 3A; Table 2). When the number of B-scans per study was then taken into account (Figure 3B; Table 2), the Zeiss Stratus was the instrument with the highest EF-scan, even compared with the Optopol Copernicus ($P = 0.005$). The Zeiss Cirrus, HRA Spectralis, and Topcon OCT had significantly lower EF-scan values than the Zeiss Stratus ($P \leq 0.001$). The Optovue RTvue-100 did not show a statistically significant difference in EF-scan compared with the Zeiss Stratus.

Error types were also evaluated for their location in the central and noncentral macula and the inner and outer retinal boundaries (Table 2). When considering all scans, there seemed to be no statistically significant difference between errors in the central and noncentral macula and more errors affecting the inner retinal boundary compared with the outer ($P = 0.006$). When considering each instrument, the HRA Spectralis tended to make more errors when delimiting the inner retina ($P < 0.001$), the Zeiss Cirrus and the Optovue RTvue-100 when delimiting the central area ($P < 0.001$ and $P = 0.01$, respectively) and inner retina ($P < 0.001$), and the Optopol Copernicus produced more errors in the segmentation of noncentral areas ($P < 0.001$) and the outer retina ($P = 0.003$). The Topcon OCT did not show significant differences in the segmentation of different macular areas or retinal boundaries.

Total errors affecting the central and noncentral macula and the inner or outer retinal boundary were also examined for each major diagnosis group (Table 3). In healthy subjects, the number of errors was higher in the noncentral macula. In the epiretinal membrane group, errors were more frequent in the

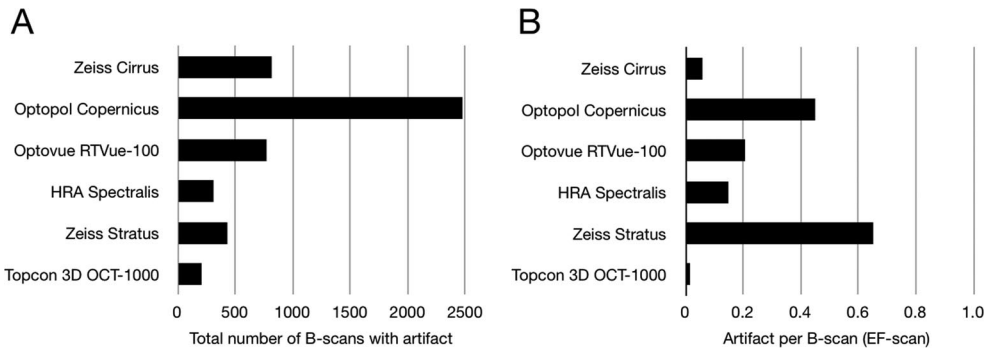

Fig. 3. Analysis of B-scan errors. **A,** Total number of errors. **B,** Total errors divided by the total number of B-scans analyzed (EF-scan). The Zeiss Stratus seemed to have a relatively low number of total errors compared with the other instruments, but when considering the number of B-scans, it had the highest EF-scan.

Table 2. Analysis Considering the Total Errors

Instruments	Total Errors	Total Errors/Total B-Scans (EF-Scan)	GLM (*P*)
Zeiss Stratus (6)*	430	0.65	—*
HRA Spectralis (19)	309	0.15	0.001
Zeiss Cirrus (128)	815	0.06	<0.001
Optopol Copernicus (50)	2,472	0.45	0.005
Optovue RTvue-100 (34)	770	0.21	0.165
Topcon 3D OCT-1000 (128)	206	0.01	<0.001
	Macular Areas: Total Errors		
	Central (1,000 μm)	Noncentral	
All	1,959	3,042	0.107
Zeiss Stratus*	182	248	—*
HRA Spectralis	103	206	0.219
Zeiss Cirrus	523	292	<0.001
Optopol Copernicus	646	1,825	<0.001
Optovue RTvue-100	433	337	0.018
Topcon OCT	72	134	0.362
	Retinal Boundary: Total Errors		
	Inner	Outer	
All	2,764	2,238	0.006
Zeiss Stratus*	158	272	—*
HRA Spectralis	272	38	<0.001
Zeiss Cirrus	560	254	<0.001
Optopol Copernicus	1,186	1,286	0.033
Optovue RTvue-100	495	275	<0.001
Topcon OCT	93	113	0.292

The number of B-scan/examination for the different instruments are given in parentheses.
*References used for GLM analysis.
GLM, generalized linear model binomial error; significant *P* values are reported.

noncentral macula and in delimiting the inner retinal boundary. In neovascular and nonneovascular AMD, the errors affecting the outer retinal boundary were more common.

Table 3. Analysis Considering Total Errors per Diagnosis

	Total Errors			
	Macular Area		Retinal Boundary	
Diagnosis	Central (1,000 μm)	Noncentral	Inner	Outer
Normal	72	560	275	358
Epiretinal membranes	516	890	1,203	203
Nonneovascular AMD	206	461	227	440
Neovascular AMD	942	791	798	935
Cystoid macular edema	223	340	261	303

The most frequent classes are reported.

Error Characterization

The errors produced by the different instruments were often similar in certain pathologic conditions. This was likely because that for all the devices, the different layers were recognized using algorithms that identified gray value variations along the A-scan lines. Pathologic hyperreflective elements can create confusion in the different instruments, leading the software to misrecognize the retinal boundaries. In particular, vitreous alterations such as partial posterior vitreous detachments or epiretinal membranes that partially adhered to the retina were problematic. The instruments often missed the inner retinal boundary identification, positioning the line on the vitreous limit (Figure 4). This generally led to overestimation of the retinal thickness.

In macular holes, the most common error was the precise recognition of hole shape, leading to overestimation of retinal thickness in the outer layers adjacent to the hole center (Figure 5). In severe myopia, the most common error was the translation of the retinal boundary adjacent to the choroid. This was the result of the significant reduction of retinal layer reflectivity and thick-

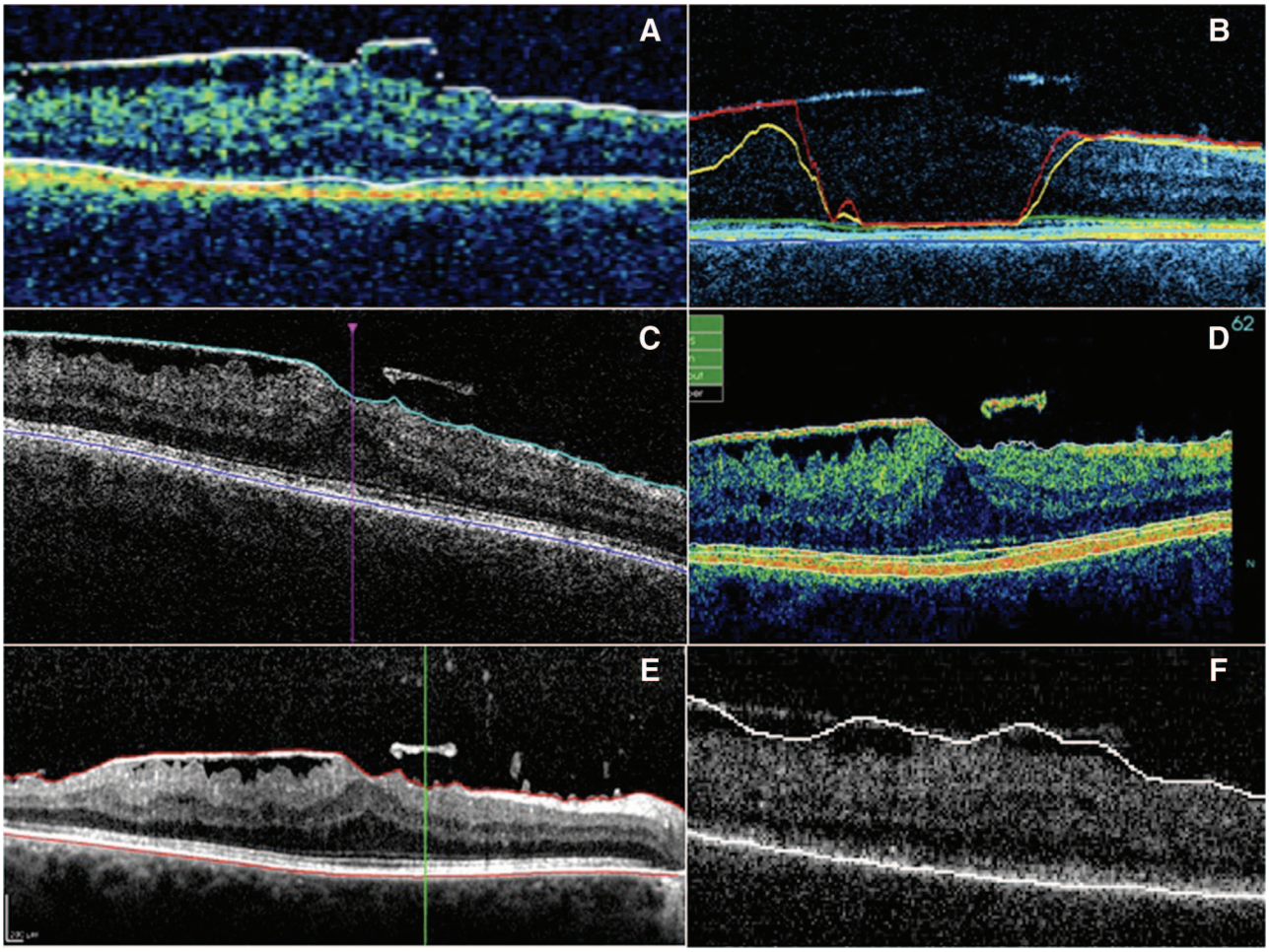

Fig. 4. Vitreoretinal traction with foveal shape alteration. **A–F,** OCT images of the same eye taken by each of the instruments. The inner retinal boundary was missed by all the instruments. The most common error was the positioning of the limit line on the vitreous hyaloid. **A,** Zeiss Stratus. **B,** Optopol OCT. **C,** Zeiss Cirrus. **D,** Topcon 3D-OCT 1000. **E,** HRA Spectralis. **F,** Optovue RTVue-100.

ness typical of this condition. The signal from the choroid was increased because of the reduced attenuation of the retina. This resulted in shifting of the boundary positions by the software toward the choroidal hyperreflectivity. In AMD with fibrotic scars, the delimitation of the outer retinal boundary was generally not precise because the OCT-generated boundary line followed the inner or outer limit of the scar. In some cases, it was set randomly inside the scar thickness.

Discussion

Optical coherence tomography is one of the most important techniques for retinal examination because it enables the preparation of histologic-like images for descriptive analysis. For systematic follow-up of different pathologic conditions, including macular edema from different origins or neurosensory and pigment epithelium detachments, the ability to quantify retinal thickness is essential.

Because of the increased speed of image acquisition, the new SD-OCT instruments are greatly improved, especially with regard to the axial resolution and quantity of information produced by a single examination. Each of these new devices has the potential to evaluate macular thickness with automated delimitation of inner and outer boundaries. However, like with the TD-OCT instruments, many types of errors can be produced that reduce the reliability of the analysis. The frequency of errors increased with the severity of retinal alteration for all the instruments in this study. There were, however, important differences among the different devices. In general, the Zeiss Cirrus, Heidelberg HRA Spectralis, and Topcon 3D OCT-1000 were the most reliable machines with excellent results, especially in normal retinas. The Zeiss Cirrus and Topcon OCT instruments use the same acquisition protocol based on 128 B-scans, each composed of 512 A-scans, which is the lowest of any in the SD-

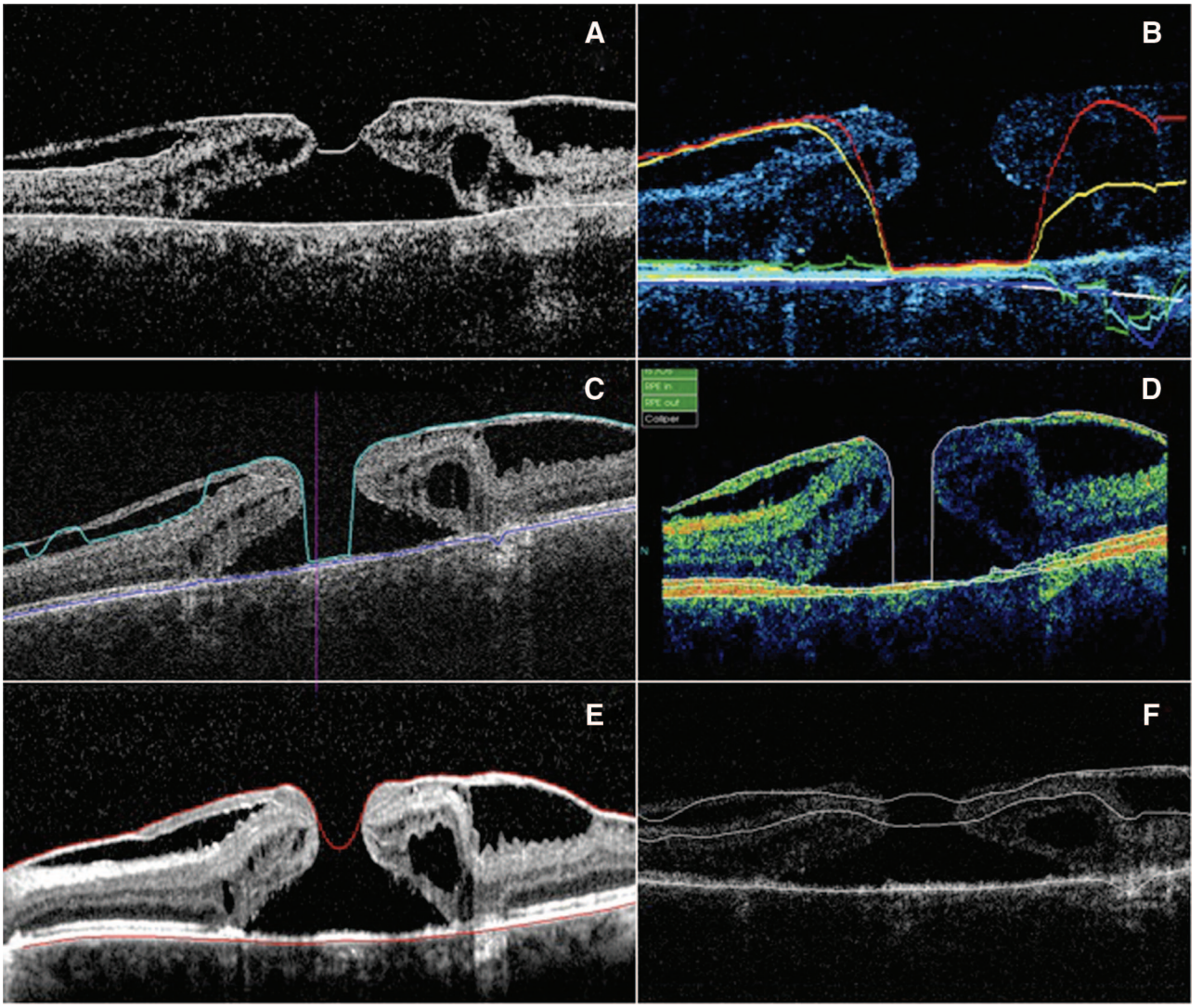

Fig. 5. A case of complete macular hole. **A–F,** OCT images of the same eye taken by each of the instruments. The identification of macular hole shape was the most frequent and relevant error for all the different algorithms. **A,** Zeiss Stratus. **B,** Optopol OCT. **C,** Zeiss Cirrus. **D,** Topcon 3D-OCT 1000. **E,** HRA Spectralis. **F,** Optovue RTVue-100.

OCT group. This implies that the effectiveness of the automated delimitation of retinal boundaries is probably not dependent on the lateral resolution.

The different protocols of analysis by the instruments produce a different number of B-scans per examination. For example, the Heidelberg Spectralis executes 19 scan lines per examination, whereas the Zeiss Cirrus produces 128. This implies that devices that use a higher number of scan lines per examination are more likely to have at least one error (EF-exam). Conversely, the Zeiss Stratus, which was the only TD-OCT system analyzed, uses a radial line protocol with six scans, and the EF-exam may not accurately describe the clinical significance. To account for these differences in acquisition protocols, the EF-scan was calculated to assess the rate of errors per individual B-scan. This was reflected in the results found for the Zeiss Stratus, which revealed a relatively low number of total artifact errors but the highest EF-scan of any instrument evaluated in this study. This suggests that the EF-scan determination may be more important when comparing the ability of different instruments to accurately create a retinal thickness map. It is acknowledged, however, that all segmentation errors as defined by the study parameters were noted without regard to potential clinical significance. Although the method of calculating the EF-scan used in this study would treat an error in accounting for a significant amount of subretinal fluid in a similar fashion to a slight breakdown of the inner retina measurement resulting from a fine epiretinal membrane, in clinical practice, the former may likely be more significant.

The position of the B-scans used by the protocols of analysis was also considered. Although all the SD-OCT systems use a raster line protocol, Stratus uses a radial line protocol, thus potentially leading to a higher number of artifacts in pathologic conditions that directly affect the fovea. Nevertheless, when comparing the errors in the central versus the noncentral area of the macula, there was no statistically significant difference for the whole sample, whereas the Zeiss Stratus produced more errors in the noncentral area, and some SD-OCT instruments such as the Zeiss Cirrus and the Optovue RTvue-100 tended to produce more errors in the central area. Furthermore, the data also suggest that errors are more likely to occur where the pathologic condition causes the most severe alteration, which means in the inner boundary in epiretinal membranes and outer boundary in the different forms of AMD (Figure 3).

The quality of the single images is directly correlated to speckle noise. This was reduced by the Heidelberg HRA Spectralis with a real-time averaging algorithm that used a variable number of single frames. Although the HRA Spectralis produced fewer errors than the TD-OCT Zeiss Stratus in pathologic conditions such as epiretinal membrane, the EF was higher compared with the Topcon 3D OCT-1000 and the Zeiss Cirrus. This implies that the error occurrence was not deeply dependent on the noise quantity. It is also possible that image quality could influence EF. A limitation of this study is that a comparison of EF with image quality was not realized, and this is because an objective and uniform quantification of OCT image quality is very difficult. Moreover, an image quality score was available for only 3 instruments, the Zeiss Stratus, Zeiss Cirrus, and Topcon 3D-OCT-1000.

All these considerations suggest that in automated retinal segmentation, the most important factor is the quality of algorithm used by the software. All the improvements provided by the SD technology are advantageous only if associated with an efficient recognition system. The Optopol Copernicus is emblematic of this issue. Even when the quality of single images was comparable with the other OCT instruments, the EF was always higher, probably as a result of a more complex analysis for retinal segmentation.

Many instruments have or will soon have the capability of manually changing the retinal boundary delimitations. This could reduce the clinical impact of OCT artifacts, but it could also introduce a significant interobserver variability that will need to be evaluated. It will also increase the time needed for the analysis of each examination. For example, with protocols that acquire at least 128 images, it would be very difficult to analyze each single frame and manually set the boundaries in all the images.

The severity of retinal abnormalities is directly connected to the frequency of errors.[1,11,14,15] This is because the software tries to identify the normal pattern of hyper- and hyporeflective layers on each single A-scan. Pathologic conditions lead to chaotic remodeling of the retinal segmentation that is strictly dependent on the severity and the type of alteration. In many cases, the error can be understood by considering the changes in reflectivity of interfaces between the different layers and lesions. For example, epiretinal membranes and partial vitreous detachments create abnormal hyperreflective bands inward of the normal retinal boundary. The algorithm identifies the abnormal bands as the retinal boundary. Under these circumstances, one should always consider the possibility of an overestimation of retinal thickness. In high myopia, the shifting of segmentation to the choroidal structure leads to unreliable examinations and invalidates the thickness measurements. In cases like this, it is suggested that decisions regarding the effectiveness of therapy should not be based on automated determinations of retinal thickness.

In conclusion, SD-OCT systems reduce, but do not eliminate, errors in automated retinal delimitation. There are important differences between the instruments studied, and manual analysis of each single B-scan used to determine the retinal thickness map can be considered. This is more important in cases in which retinal shape is deeply disrupted. In the most severe situations, it is suggested that the automatically generated retinal thickness values should not be used for diagnostic decision-making. The algorithms used by the OCT instruments are always in evolution and become better with each new software version release. Thus, it is likely that similar studies using the next algorithms will reveal lower percentages in erroneous examination.

Key words: artifacts, comparison, optical coherence tomography, retinal boundaries, retinal segmentation, spectral domain.

References

1. Leung CK, Chan WM, Chong KK, et al. Alignment artifacts in optical coherence tomography analyzed images. Ophthalmology 2007;114:263–270.
2. Hee MR, Izatt JA, Swanson EA, et al. Optical coherence tomography of the human retina. Arch Ophthalmol 1995;113: 325–332.
3. Huang D, Swanson EA, Lin CP, et al. Optical coherence tomography. Science 1991;254:1178–1181.
4. Puliafito CA, Hee MR, Lin CP, et al. Imaging of macular diseases with optical coherence tomography. Ophthalmology 1995;102:217–229.

5. Swanson EA, Izatt JA, Hee MR, et al. In vivo retinal imaging by optical coherence tomography. Opt Lett 1993;18:1864–1866.
6. Thomas D, Duguid G. Optical coherence tomography—a review of the principles and contemporary uses in retinal investigation. Eye 2004;18:561–570.
7. Apushkin MA, Fishman GA, Janowicz MJ. Monitoring cystoid macular edema by optical coherence tomography in patients with retinitis pigmentosa. Ophthalmology 2004;111:1899–1904.
8. Browning DJ, McOwen MD, Bowen RM Jr, O'Marah TL. Comparison of the clinical diagnosis of diabetic macular edema with diagnosis by optical coherence tomography. Ophthalmology 2004;111:712–715.
9. Larsson J, Zhu M, Sutter F, Gillies MC. Relation between reduction of foveal thickness and visual acuity in diabetic macular edema treated with intravitreal triamcinolone. Am J Ophthalmol 2005;139:802–806.
10. Muscat S, Srinivasan S, Sampat V, Kemp E, Parks S, Keating D. Optical coherence tomography in the diagnosis of subclinical serous detachment of the macula secondary to a choroidal nevus. Ophthalmic Surg Lasers 2001;32:474–476.
11. Karam EZ, Ramirez E, Arreaza PL, Morales-Stopello J. Optical coherence tomographic artifacts in diseases of the retinal pigment epithelium. Br J Ophthalmol 2007;91:1139–1142.
12. Pons ME, Garcia-Valenzuela E. Redefining the limit of the outer retina in optical coherence tomography scans. Ophthalmology 2005;112:1079–1085.
13. R Development Core Team. R: A language and environment for statistical computing; 2005. ISBN: 3-900051-07-0, available at: www.R-project.org. Accessed October 20, 2009.
14. Ray R, Stinnett SS, Jaffe GJ. Evaluation of image artifact produced by optical coherence tomography of retinal pathology. Am J Ophthalmol 2005;139:18–29.
15. Sadda SR, Wu Z, Walsh AC, et al. Errors in retinal thickness measurements obtained by optical coherence tomography. Ophthalmology 2006;113:285–293.
16. Wojtkowski M, Bajraszewski T, Gorczynska I, et al. Ophthalmic imaging by spectral optical coherence tomography. Am J Ophthalmol 2004;138:412–419.
17. Wojtkowski M, Leitgeb R, Kowalczyk A, Bajraszewski T, Fercher AF. In vivo human retinal imaging by Fourier domain optical coherence tomography. J Biomed Opt 2002;7:457–463.